Original
Received December 23, 2005
Accepted for Publication July 27, 2006

Material Flow and the Shear Layer in the Upper Weld Zone during Friction Stir Welding of Aluminium Alloys

Z.W.CHEN, R.PERIS, R.MAGINNESS and Z.XU

ERI, School of Engineering, Auckland University of Technology, NZ
Zhan.chen@aut.ac.nz

Friction stir welding (FSW) experiments were conducted using three different aluminium alloys (a work hardened alloy, an age hardened alloy and a cast alloy) followed by metallographic examination focusing on the upper weld zone and the surface layer. The examination has revealed the features of the major forward flow resulting from the forward motion of the tool shoulder. A thin shear layer due to tool rotation was identified between the tool shoulder and the workpiece with a distinctive shear flow direction. The thickness of the shear layer was alloy dependent. An embedded layer in the upper weld zone has also been identified. The flow phenomena leading to this will be discussed. A velocity profile in the shear layer, based on the apparent alignment of Si particles in the cast alloy after welding, has suggested a dominant sliding contact condition.

Key Words : Friction stir welding, tool shoulder, flow, shear layer ; contact condition

1. INTRODUCTION

Friction stir welding (FSW), which is a relatively new solid-state joining technology, has in the last few years increasingly been introduced and implemented in many industries in the world, particularly in Japan. At the same time, there have been a number of experimental studies focusing on the material flow during FSW, particularly on the formation of weld nugget zones [1-8]. The upper weld zone is primarily the result of the interaction between the workpiece and the tool shoulder but the detailed forming mechanism is yet to be fully determined [7].

Research on FSW has recently been the subject of a thorough review by Mishra and Ma [9] and it was concluded that the complex phenomena of material flow during FSW is still poorly understood. Nelson [10], in another recent review on FSW, pointed out that the physics of the tool/workpiece interface, which is currently not understood, is primarily important for understanding many aspects of FSW particularly material flow.

As the name of the process implies, friction is a very important feature of the process. However, the tool-workpiece contact conditions are currently not certain [11]. The nature of the shear layer and the tool-workpiece contact conditions are primarily important for developing analytical models [12,13] and numerical analysis for the understanding of the flow phenomena of FSW [14].

In this study, FSW experiments were conducted using three different aluminium alloys to order to provide different flow marking characteristics. After analyzing the structures, material flow in the upper weld zone is suggested and the nature of the shear layer is described.

2. EXPERIMENTAL PROCEDURES

For FSW, a Lagun milling machine was used and the relative movement of the tool and the workpiece (aluminium alloy plate) during FSW ($\omega = 800$ rpm) is illustrated in Figure 1. The ends of the plate were clamped onto the milling machine bed with a steel plate backing (not shown in Figure 1).

Aluminium alloy 5083 (Al-4.5Mg-0.6Mn) rolled plates (6 mm thick), 6060 (Al-0.5Mg-0.5Si) flat bars (6 mm thick) and A356 (Al-7Si-0.3Mg) cast alloy (machined to 6 mm thick from ingots) were used. A micrograph of the cast alloy is given Figure 2, showing Al-Si eutectic in an interdendritic region and Si particles largely in an elongated and fibrous form. We used this alloy as we intended to evaluate whether the deformation patterns of dendrites and eutectic Al-Si could act as short-distance flow markers.

FSW tools (with lefthand-thread pins) were machined using

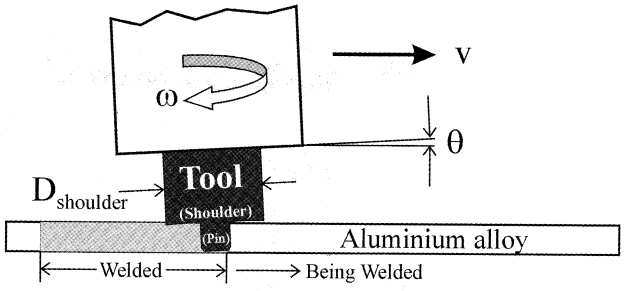

Figure 1 Schematic illustrating friction stir welding and the controlling parameters.

tool steel. Two values of $D_{shoulder}$ were used, 20 and 16 mm. D_{pin} was 6 mm and v = 1 mm/s for FSW of 5083 alloy and 5083/6060 alloy. For the cast alloy, a much higher velocity could be used and in this paper results presented are based on using a velocity of 3 mm/s. Pin length was 5.5 mm for both cases (for FSW of both wrought and cast alloys). Temperature measurement was also made by placing K-type thermocouples in 1 mm diameter holes in weld plates (mid-thickness locations). After welding, samples were prepared for examination following the normal metallography procedure.

3. RESULTS END DISCUSSION

3.1 Material flow

In presenting images of the transverse cross sections of the welds below, the advancing side of the weld is always on the right. The side of the weld is referred to as advancing side where the rotation motion (clock wise) of the tool is in the same direction as the welding direction. The other side of the weld, where the rotation motion of the tool is in opposite direction to the welding direction, is referred to as retreating side.

A transverse cross section of the 5083 alloy weld made using $D_{shoulder}$ = 20 mm is shown in Figure 3 showing the typical weld nugget with the ring pattern. Note that there is a line appeared white, pointed to by the arrow, and in 3D it should be a layer in the upper weld zone. We name this layer as embedded layer.

Temperatures detected using thermocouples are plotted in Figure 4. The curve with the thermocouple placed originally inside the weld zone area (0 mm curve) was interfered by the stir action of the material flow but a peak temperature of 565℃ was detected. This temperature is lower than the liquidus of the alloy.

When the small $D_{shoulder}$ (16 mm) was used for 5083 alloy, FSW resulted in a continuous lack of join, forming a channel type defect along the whole weld in the upper weld zone, as shown in Figure 5a. This defected weld, however, has revealed the major material flow in that zone, as indicated in Figure 5b. On the surface of this major flow, there is a thin shear layer (appearing white in Figure 5a and black in Figure 5b). A significant amount of the sheared material accumulated in the flow front (Figure 5) presumably as a result of the material having been sheared off by the shoulder and deposited onto the flow front (free surface).

It is clear from Figure 5 that the flow in the upper zone is dominated by the flow from retreating side to the advancing side (denoted as d_{R-T}). This flow was however not extensive in this worked hardened alloy, as the original rolled structure was almost unaltered, although continuously being locally curved in the flow

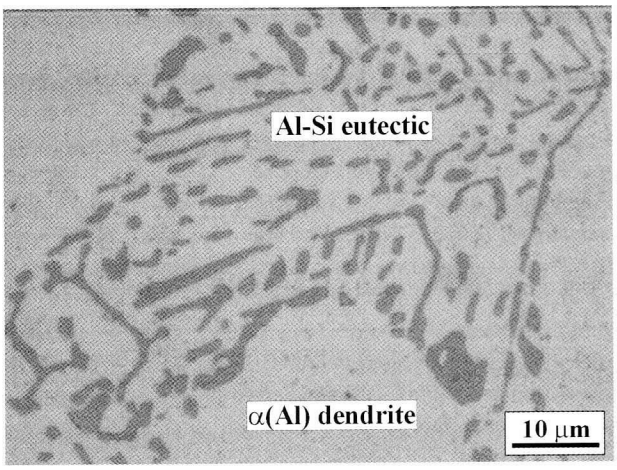

Figure 2 Microstructure of A356 cast alloy.

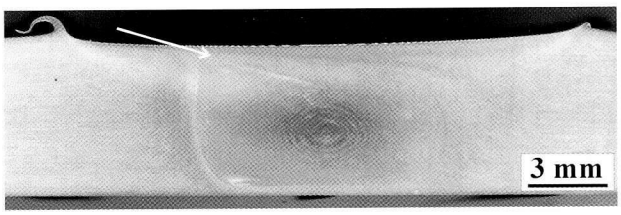

Figure 3 Cross section of alloy 5083 weld (advancing side on the right) made using $D_{shoulder}$ = 20 mm and $\theta = 2^\circ$ Arrow points to "embedded layer".

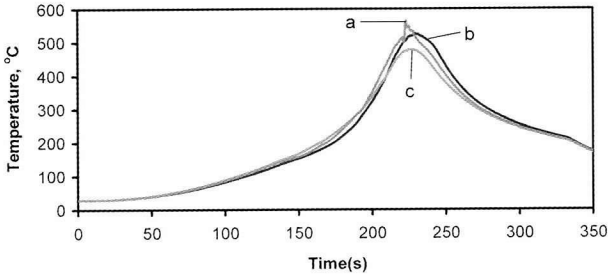

Figure 4 Temperature curves with distance of thermo-couple from centre : 0 mm for curve a, 4 mm for curve b and 10 mm for curve c. Weld was made using alloy 5083 and $D_{shoulder}$ = 20 mm and $\theta = 2^\circ$.

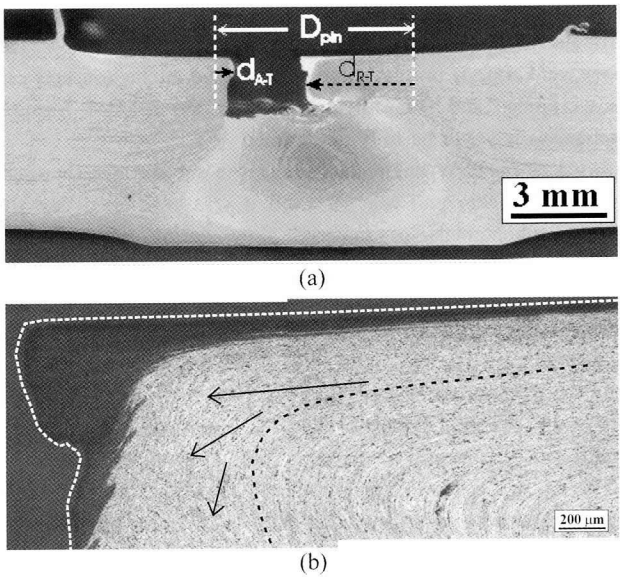

Figure 5 Cross section of alloy 5083 weld made using $D_{shoulder}$ = 16 mm and $\theta = 2^\circ$. d_{R-T} and d_{A-T} represent flows from retreating side and advancing side, respectively. Micrograph in (b) was taken in d_{R-T} region as shown in (a). In (b), the black dotted curve indicates the original rolled structure/direction and arrows indicate suggested local flow directions during FSW.

front, as shown in Figure 5b.

Examining the end of the weld (Figure 6) has given a better understanding of the flow in the upper zone. During FSW, the shoulder, which is tilted, forged the flow in the upper zone from point 1 to point 2, for a distance, $d_{R\text{-}Net}$. This flow can be viewed as the combination of two flows, the forward flow (for a distance d_F), and the flow in the direction transverse to the welding (forward) direction (for a distance $d_{R\text{-}T}$). As shown in Figure 5, the transverse flow was predominantly from the retreating side, meaning $d_{R\text{-}T} >> d_{A\text{-}T}$), due to the effect of the top shear layer (due to the rotating shoulder).

The use of a higher tilt angle increased the amount of the flows in the upper zone, not only from the retreating side ($d_{R\text{-}T}$) but also from the advancing side ($d_{A\text{-}T}$), as shown in Figure 7. This suggested again that the flow in the upper zone was primarily influenced by the shoulder forging (forward) function. The increased flow volume resulted in a near closure of the channel, with a section of the shear layer embedded.

The major flow in the upper weld zone mainly caused by the forward motion of (forged by) the tool shoulder can be further illustrated by FSW of 5083/6060 plates (Figure 8). When 6060 plate was placed on the retreating side, the major flow ($d_{R\text{-}Net}$) was usual so that flow distance $d_{R\text{-}T}$ dominated, as shown in Figure 8a.

However, when 5083 plate was placed on the retreating side, flow from the retreating side ($d_{R\text{-}T}$) no longer dominated. Instead, a flow from the advancing side ($d_{A\text{-}T}$) was significant, although the flow direction in this case was opposite the rotating direction of the shoulder. This unusual flow can be understood by examining the plasticity of the alloys using the Zener-Hollomom parameter, relating equivalent flow stress (σ) to equivalent strain rate ($\dot{\varepsilon}$) at temperature T [15]:

$$Z = A(\sinh\ \alpha\sigma)^n = \dot{\varepsilon}\exp\left(\frac{Q_{HW}}{RT}\right) \quad (1)$$

where A, α, n are materials constants and Q_{WH} is the activation energy for deformation (hot working) and R is the universal gas constant.

Using the available data [15] and a temperature at 565℃ (Figure 4), we have for 5083 alloy:

$$\dot{\varepsilon} = 0.22(\sinh 0.015\sigma)^{4.99}\ s^{-1} \quad (2)$$

and for 6063 alloy:

$$\dot{\varepsilon} = 8.8(\sinh 0.04\sigma)^{5.39}\ s^{-1} \quad (3)$$

Data for 6060 alloy was not given [15]. Alloy 6060 is similar to 6063, both classified as alloys with high extrudability. However, the level of Mg in 6060 is lower and hence a higher extrudability is expected [15].

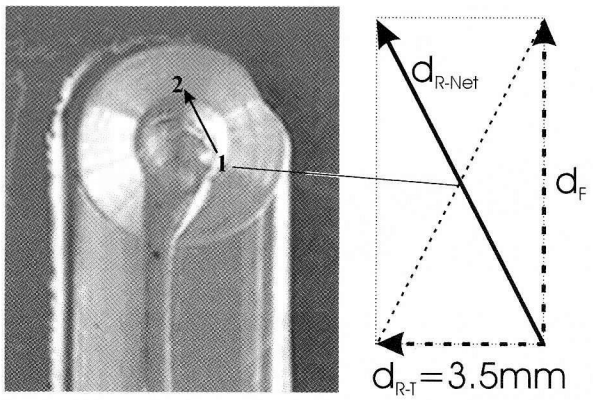

Figure 6 Top view of alloy 5083 (end) weld made using $D_{shoulder}$=16 mm and θ=2°, indicating flow $d_{R\text{-}Net}$ as a combination of the flows, d_F and $d_{R\text{-}T}$.

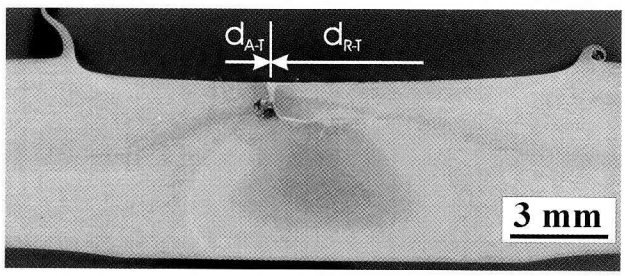

Figure 7 Cross section of alloy 5083 weld made using $D_{shoulder}$=16 mm and θ=3°.

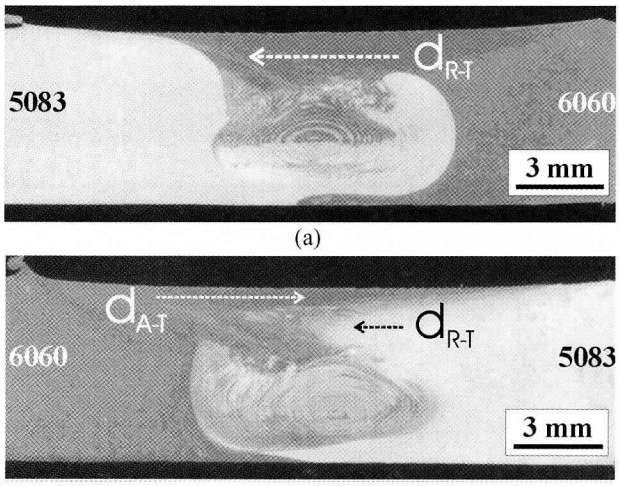

Figure 8 Cross sections of (a) 5083/6060 and (b) 6060/5083 welds (advancing side on right) made using $D_{shoulder}$=20 mm and θ=2° (flows indicated by arrows).

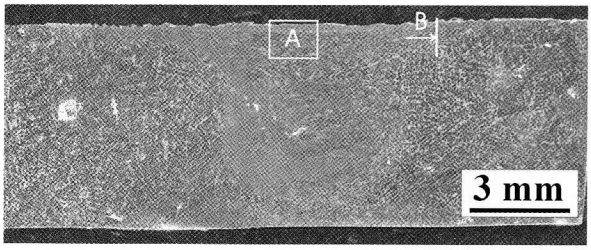

Figure 9 Cross section (advancing side on the right) of cast A356 alloy weld made using $D_{shoulder}$=16 mm and θ=2°. Locations A (transverse) and B (longitudinal) are where metallographic examination was made and micrographs are given later in the following section.

From equations (2) and (3), we can expect that the plastic flow is considerably more extensive for alloy 6060 than 5083, under the same flow stress. Hence, it is reasonable for a high d_{A-T} value when 6060 was placed in the advancing side, as shown in Figure 8b. This further illustrates that forward forging provided by the shoulder is the dominant deformation and material flow in the upper weld zone.

Material also flowed readily using the as-cast A356 alloy and a complete weld was achieved using $D_{shoulder} = 16$ mm and at a significantly higher travel speed at 3 mm/s (Figure 9). It is evident that dendrites, although deformed, can be seen in the upper weld zone, except in the shear (and the embedded) layer. This indicates that deformation in the upper zone was not extensive (but enough to close the channel) to completely alter the original microstructure, except in the shear layer.

3.2 Shear layer

Micrographs taken in location A in Figure 9 of the A356 alloy weld are shown in Figure 10. It is clear that dendrites were compressed, except in the top 150-200μm shear layer where original dendrites could no longer be identified. Material in the shear layer has been heavily deformed that the original dendritic appearance has totally disappeared. Instead shear direction in the shear layer can be identified (as indicated by arrows for a velocity profile in Figure 10b).

Observation on a longitudinal cross section (location B in Figure 9) was made, as shown in Figure 11. It is clear that dendrites have been compressed (secondary dendrite arm spacing has become smaller) and forged/bent towards the welding direction. The microstructure of the shear layer is consistent with that observed in the transverse cross section (Figure 10b). The shear direction is, however, not clear in Figure 11b because the shear direction during FSW was almost normal to this longitudinal cross section and also near normal to the major flow (due to forging) direction in the upper zone. Hence, there is no clear shear direction in this plane of observation.

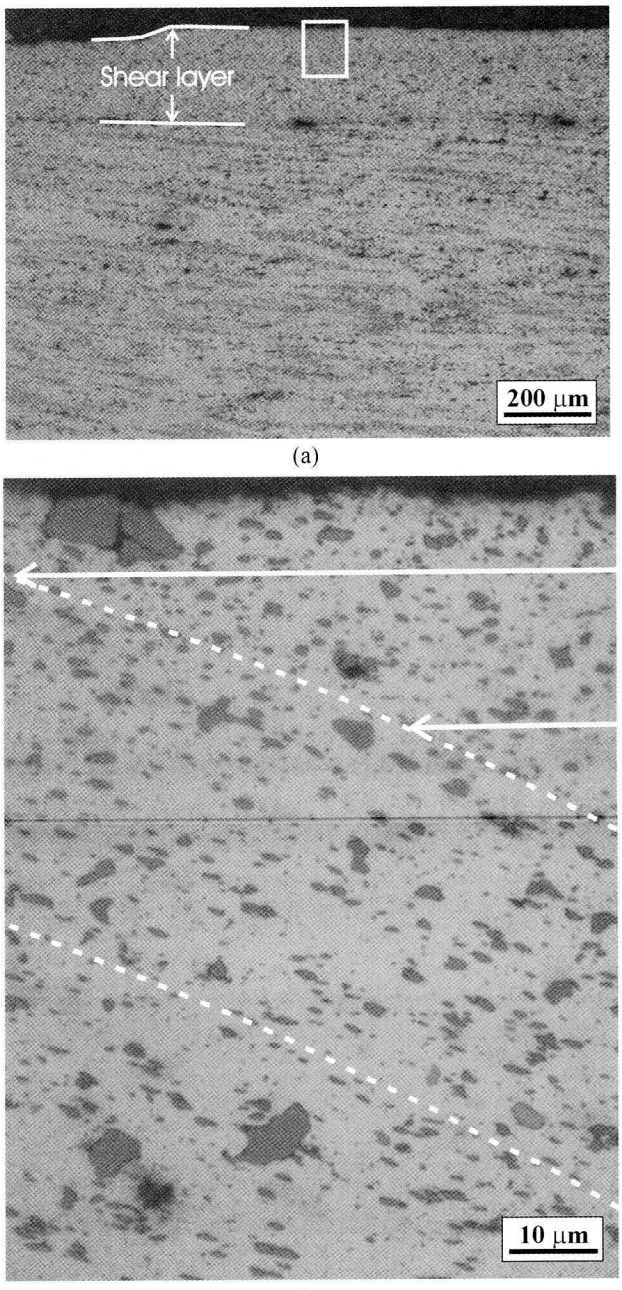

Figure 10 Micrographs taken in location A as indicated in Figure 9, (a) lower magnification and (b) high magnification in the shear layer. Arrows suggest relative flow velocities.

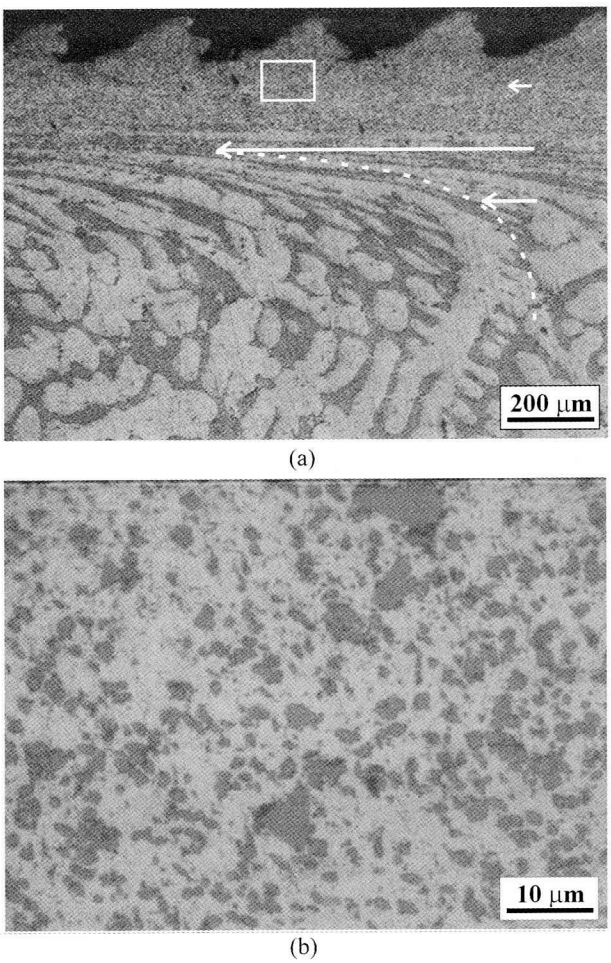

Figure 11 Microstructure of the weld in retreating side observed in the longitudinal cross section of A356 alloy weld (sample taken in location B as indicated in Figure 9). Arrows suggest relative velocities.

The thickness of the shear layer was alloy dependent. For 5083 work hardened alloy, the layer under the shoulder was thin, up to 50μm, except in the flow front where the sheared off material built up. For A356 cast alloy, the layer thickness was 150-200μm, depending on location. It is likely that the thickness increases with the plasticity of the workpiece.

The peak temperature of ~565° (Figure 4) is just below the Al-Si eutectic temperature and hence Al-Si eutectic melting should not occur. Si particles in the shear layer (Figsure 10 and 11) after FSW were similar to those in the original eutectic regions (Figure 2). The difference was the fragmentation of the more elongated Si particles (in the as-cast state) during FSW. Shear deformation caused Si particles realignment due to the local velocity difference. Therefore, the alignment of the Si particles after FSW could suggest a velocity field.

The indicative velocity field shown in Figure 12 (also Figure 10b) suggests a shear strain slightly higher than 3. Taking the shear layer thickness as 0.2 mm, the relative movement (between the top and the bottom of the shear layer) was then in the order of 0.6 mm. We consider a rotation speed 800 rpm, a location of 5 mm from the tool centre (D=10 mm), travel speed 3 mm/s and a fully sticking condition (meaning that the workpiece surface contacting the tool shoulder will travel the same speed as the tool). A contact point should then have traveled more than 500 mm (instead of ~ 0.6 mm). Hence, sticking condition was not established in the present experimental conditions. This is in a disagreement to the suggested sticking condition prevailing during FSW [16].

4. Conclusions

The major (forward) flow in the upper weld zone was the result of the workpiece having been forged forward by the tool shoulder. Shearing between the tool shoulder and the workpiece due to rotation of the tool resulted in the formation of a shear layer. The thickness of the shear layer was alloy dependent, ranging from 200μm for the cast alloy to being ~ 50μm for the work hardened alloy. In a sound weld, a section of the shear layer was "lowed" over, becoming an embedded layer. It appears that the shear deformation in the shear layer was too low to suggest a sticking condition prevailing at the tool-workpiece interface.

Acknowledgments The authors would like to sincerely thank Professor R. Geddes and Mr. P. Foreman for their support on our FSW research, Mr. R. Reichardt for assisting in FSW experiments. One of the authors (ZWC) would also like to sincerely thank Professor O. Kamiya, Professor H. Kokawa and Dr. Y. Sato for introducing him to FSW.

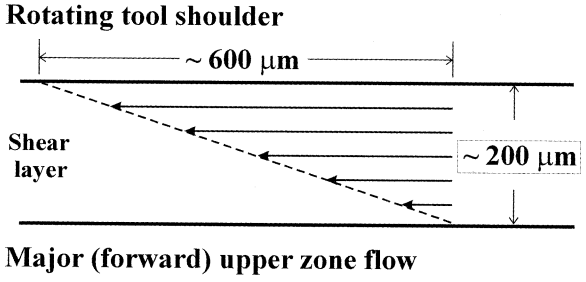

Figure 12 Suggested velocity (flow distance) field in the shear layer, based on microstructure given in Figure 10b.

References

[1] Colligan, K., "Material flow behavior during friction stir welding of aluminium", Weld. J., Vol.78, pp.229s-237s, (1999).
[2] Li, Y., Murr, L.E. and McClure, J.C., "Flow visualization and residual microstructures associated with the friction-stir welding of 2024 aluminium to 6061 aluminium", Mater. Sci. Eng., Vol. A271, pp.213-223, (1999).
[3] Sutton, M.A., Yang, B., Reynolds, A.P. and Taylor, R., "Microstructural studies of friction stir welds in 2024-T3 aluminium", Mater. Sci. Eng., Vol.A323, pp.160-166, (2002).
[4] Krishnan, K.N., "On the formation of onion rings in friction stir welds", Mater. Sci. Eng., Vol. A327, pp.246-251 (2002).
[5] Lee, W.B., Yeon, Y.M. and Jung, S.B., "The joint properties of dissimilar formed Al alloys by friction stir welding according to the fixed location of materials", Scr. Meter., Vol.49, pp.423-428, (2003).
[6] Wert, J.A., "Microstructures of friction stir weld joints between an aluminium-base metal matrix composite and a monolithic aluminium alloy", Scri. Meter., Vol.49, pp.607-612, (2003).
[7] Guerra, M., Schmidt, C., McClure, J.C., Murr, L.E. and Nunes, A.C., "Flow patterns during friction stir welding", Mater. Charact., Vol.49, pp.95-101, (2003).
[8] Ke, L., Xing, L. and Indacohea, J.E., "Material flow patterns and cavity model in friction-stir welding of aluminium alloys", Metall. Mater. Trans., Vol.35B, pp.153-160, (2004).
[9] Mishra, R.S. and Ma, Z.Y., "Friction stir welding and processing", Mater. Sci. Eng. Rep., Vol.50, pp.1-78, (2005).
[10] Nelson, T.W., in Friction Stir Welding and Processing III, San Francisco, Edited by Jata et al., TMS, Warrendale, pp.149-159, (2005).
[11] Colegrove, P.A. and Shercliff, H.R., "3-dimentional CFD modeling of flow round a threaded friction stir welding tool profile", J. Mater. Process. Technol., Vol.169, pp.320-327, (2005).
[12] Schmidt, H., Hattel, J. and Wert, J., "An analytical model for the heat generation in friction stir welding", Model. Simul. Mater. Sci. Eng., Vol.12, pp.143-157, (2004).
[13] Schmidt, H., Hattel, J., "A local model for the thermomechanical conditions in friction stir welding", Model. Simul. Mater. Sci. Eng., Vol.13, pp.77-79, (2005).
[14] Schmidt, H., Hattel, J., "Modelling heat flow around tool probe in friction stir welding", Sci. Technol. Weld. Joining, Vol.10, pp.176-186, (2005).
[15] Sheppard, T., "Extrusion of Aluminium Alloys", Kluwer Academic Publishers, Dordrecht, (1999).
[16] Yan, J., Sutton, M.A. and Reynolds, A.P., in Proceedings of the 5th International Friction Stir Welding Symposium, Metz, 2004 (CD-ROM).